References

ALCOCK, N. W., ESPERAS, S., BAGNALL, K. W. & HSIAN-YUN, W. (1978). *J. Chem. Soc. Dalton Trans.* pp. 638–646.
BEINEKE, T. A. & DELGAUDIO, J. (1968). *Inorg. Chem.* 7, 715–721.
BROWN, D. (1973). *Comprehensive Inorganic Chemistry*, pp. 286–304. Oxford: Pergamon Press.
Enraf–Nonius (1986). *Structure Determination Package*. Version 18. Enraf–Nonius, Delft, The Netherlands.

JOHNSON, C. K. (1976). *ORTEPII*. Report ORNL-5138. Oak Ridge National Laboratory, Tennessee, USA.
KHAN, M. A., KUMAR, N. & TUCK, D. G. (1984). *Can. J. Chem.* 62, 850–855.
REBIZANT, J., APOSTOLIDIS, C., SPIRLET, M. R., ANDREETTI, G. D. & KANELLAKOPULOS, B. (1988). *Acta Cryst.* C44, 2098–2101.
ŠĆAVNIČAR, S. & PRODIĆ, B. (1965). *Acta Cryst.* 18, 698–702.

Single-Crystal Structure of BaSm2S4

BY JAMES D. CARPENTER AND SHIOU-JYH HWU*

Department of Chemistry, Rice University, PO Box 1892, Houston, Texas 77251, USA

Abstract. Nonstoichiometric barium samarium sulfide, $Ba_{1-x}Sm_2S_{4-x}$ ($x = 0.10$), $M_r = 549.43$, orthorhombic, *Pnma*, $a = 12.262$ (3), $b = 4.121$ (3), $c = 14.713$ (2) Å, $V = 743.5$ (6) Å^3, $Z = 4$, $D_x = 4.91$ g cm^{-3}, λ(Mo $K\alpha$) = 0.71069 Å, $\mu = 218.74$ cm^{-1}, $T = 296$ K, $F(000) = 947.2$, $R = 0.027$, $wR = 0.037$ for 736 observed unique reflections [$I > 3\sigma(I)$]. X-ray single-crystal structure results confirm that the title compound crystallizes in a $CaFe_2O_4$-type structure, which is built up from edge-sharing, double octahedral, infinite chains. The structure also contains BaS_8 polyhedra, which can best be described as bicapped trigonal prisms (b.t.p). The two capping S(2) atoms adopt much longer Ba—S bond distances. This is attributed in part to the nonstoichiometry of the Ba and S(2) site. The same structure type is also adopted by other heavier rare-earth metal ternary sulfides and selenides, *e.g.*, $A(RE)_2Q_4$ ($Q = S$ and Se), where RE = Tb—Lu for $A = Sr$ and RE = Nd–Lu for $A = Ba$.

Introduction. The combination of alkaline-earth (*A*) and rare-earth (RE) chalcogenides (*Q*) allows for the formation of a series of ternary compounds with a general formula of $A(RE)_2Q_4$, where $A = Sr$, Ba; RE = La–Lu, and $Q = S$, Se (Patrie, Golabi, Flahaut & Domange, 1964). These ternary rare-earth chalcogenide compounds appear in different structure types, *e.g.* $CaFe_2O_4$ (Decker & Kasper, 1957) and Th_3P_4 (Meisel, 1939). It is recognized that the coordination of the trivalent rare-earth cations, $(RE)^{3+}$, governs the formation of each specific structure type. Patrie *et al.* have prepared a series of polycrystalline samples of ternary strontium and barium rare-earth

sulfides and selenides. They observed, using indexed powder X-ray diffraction patterns, that the ternary phases which incorporate rare-earth elements at the end of the lanthanide series possess the $CaFe_2O_4$-type structure. Due to a lack of a single crystal, no structure characterization has been made. We report the X-ray single-crystal structure of $BaSm_2S_4$, which provides the detailed atomic arrangements and bond interactions for the late series of the ternary rare-earth sulfides and selenides. Nonstoichiometry due to cation deficiency, found during the single-crystal investigation of $Ba_{1-x}Sm_2S_{4-x}$, is reported for the first time and is also discussed.

Experimental. *Synthesis and crystal growth.* Single crystals of $BaSm_2S_4$ were discovered in the reaction products formed during an attempt to synthesize the '$BaSmInS_4$' analogue of $CaYbInQ_4$ ($Q = S$ and Se) (Carpenter & Hwu, 1991) using a halide flux. For the preparation of the quaternary precursor a solid-state reaction, using the starting materials BaS (Aesar 99.9%), Sm (Aldrich 99.9%), In (Aldrich 99.98%), and S (Aldrich 99.99%) in a molar ratio of 1:1:1:3, was carried out. The reaction mixture was ground together under a blanket of nitrogen in a dry box and then loaded into a quartz reaction ampule, which was subsequently sealed under vacuum. The reaction mixture was heated stepwise to a final temperature of 1223 K, annealed at this temperature for two days, and then cooled to room temperature over a 24 h period. To prepare the flux, $BaCl_2$ (Mallinckrodt, reagent) and KCl (Baker, reagent) were dried under vacuum at approximately 473 K, weighed in a dry box, and ground together prior to use. The composition of the eutectic flux was $BaCl_2$:KCl ~ 28:72 mol % (m.p. 923 K) obtained

---

* To whom all correspondence should be addressed.

from *Phase Diagrams for Ceramists* (1969). Crystal growth experiments were carried out in carbon-coated silica ampules, which were previously out-gassed under vacuum. The ampules were loaded in a dry box with a mixture of the precursor and flux in a mass ratio of 1:4. The loaded ampules were held under active vacuum for 2.5 h prior to sealing. The crystal growth reaction mixture was heated to 1268 K at a rate of approximately 30 K h^{-1}, held at 1268 K for six days, cooled at a rate of 1.5 K h^{-1} to 873 K, and then cooled to room temperature over a 24 h period. Red, transparent, needle crystals of BaSm$_2$S$_4$ were removed from the flux by washing the product with deionized water.

Structure determination. A needle-shaped crystal, with dimensions $0.5 \times 0.1 \times 0.1$ mm, was selected for indexing and intensity data collection. Diffraction data were collected using a Rigaku AFC5S four-circle diffractometer equipped with a graphite mono-chromator. The unit-cell parameters and the orientation matrix for data collection were determined by least-squares fit of 25 peak maxima ($8 < 2\theta < 23°$). There was no detectable decay of the intensities of three standard reflections (320, 220, 121) which were measured every 150 reflections during data collection. A unique data set ($0 \leq h \leq 15, 0 \leq k \leq 19, 0 \leq l \leq 5$) was collected using an ω scan with a scan speed of $4.0° \min^{-1}$ and a scan range of $\pm 0.45°$ in ω, and $2\theta_{max} = 55°$. 950 reflections were measured, of which 736 reflections [$I > 3\sigma(I)$] were used to solve and refine the structure. The *TEXSAN* (1989, version 2.0) software package was used for data reduction, intensity analysis, and space-group determination. On the basis of the intensity statistics as well as the success-ful solution and structure refinement, the space group was determined to be *Pnma* (No. 62). The following matrix was used to transform the cell to its standard setting:

$$\begin{pmatrix} 1 & 0 & 0 \\ 0 & 0 & 1 \\ 0 & -1 & 0 \end{pmatrix}.$$

Lorentz–polarizaton and empirical absorption corrections (relative transmission range: 0.67–1.00) based on two azimuthal scans ($2\theta = 10.27$ and $19.85°$) were applied to the intensity data. The atomic coordinates were found using the same soft-ware package. A correction for secondary extinction ($\Delta F / \sigma F > 10$ for reflection 020 before the correction) was applied [$2.8 (4) \times 10^{-7}$]; $|F_c| = K^{-1}|F_o|[X^* + (1 + X^{*2})^{1/2}]^{1/2}$, X^* is the value of X corresponding to a replacement of $|F_c|$ by $K^{-1}|F_o|$ (Zachariasen, 1968). The structure and thermal parameters were refined stoichiometrically by full-matrix least-squares methods, $\Sigma w(|F_o| - |F_c|)^2$, $w = [\sigma^2(F_o)]^{-1}$ ($\sigma^2 =$ variance), including 44 variables, to $R = 0.034$, $wR =$

Table 1. *Positional and thermal parameters for* Ba$_{1-x}$Sm$_2$S$_{4-x}$ ($x = 0.10$)

Anisotropically refined atoms are given in the form of the isotropic equivalent displacement parameters defined as $B_{eq} = (8\pi2/3)$ trace U.

	x	y	z	$B_{eq}(\text{Å}^2)$
Ba*	0.24529 (8)	¼	0.16007 (6)	0.95 (3)
Sm(1)	0.07608 (6)	¼	0.89625 (5)	0.83 (3)
Sm(2)*	0.07411 (6)	¼	0.39223 (5)	0.97 (3)
S(1)	0.3691 (3)	¼	0.5230 (2)	1.3 (1)
S(2)	0.4829 (3)	¼	0.2824 (2)	0.8 (1)
S(3)	0.0783 (3)	¼	0.5800 (2)	1.3 (1)
S(4)	0.2898 (3)	¼	0.8269 (3)	1.3 (1)

* Independently refined multiplicities are 0.457 (2) for Ba and 0.450 (6) for S(2) (see text).

0.051, and GOF = 1.81. The occupancy factors for all the atoms were initially refined but the resultant values indicated nonstoichiometry only on Ba and S(2) sites. The final refinement with varied occupancy factors for Ba and S(2) atoms resulted in significantly improved values of $R = 0.027$, $wR = 0.037$, GOF = 1.30, $(\Delta/\sigma)_{max} = 0.01$, $(\Delta\rho)_{min} = -3.63$, and $(\Delta\rho)_{max} = 2.64$ e Å^{-3} for 46 variables. A correction for secondary extinction [$3.1 (3) \times 10^{-7}$] was simultaneously applied. It is noted that nonstoichiometry is a phenomenon frequently observed in the $A(RE)_2Q_4$ series (Carpenter & Hwu, 1992). Single-crystal investigations have shown that this phenomenon appears in different forms; *i.e.* nonstoichiometry can be attributed to cation mixing, *e.g.*, Ca$_{1-x}$Yb$_{2+x}$S$_4$, or to cation and anion deficiency, *e.g.*, as seen in the title compound Ba$_{1-x}$Sm$_2$S$_{4-x}$. For the convenience of structural illustration the stoichiometric structural formula, BaSm$_2$S$_4$, is used hereafter. The final positional and thermal parameters are given in Table 1. Scattering factors: *International Tables for X-ray Crystallography* (Cromer & Waber, 1974).†

Discussion. The title compound crystallizes in an orthorhombic unit cell. This ternary barium samarium sulfide, BaSm$_2$S$_4$, has the CaFe$_2$O$_4$ structure with Ba^{2+} cations in positions of eight-coordination and Sm^{3+} cations in positions of six-coordination. Fig. 1 shows the contents of a unit cell, as viewed approximately along the *b* axis. The unit cell is slightly tilted so that the octahedrally coordinated SmS$_6$ may be discerned. Two Sm(1)S$_6$ octahedra, centered around the inversion center at ($\frac{1}{2}, \frac{1}{2}, \frac{1}{2}$), share a set of two S atoms, 2 S(1), while the neighbouring Sm(2)S$_6$ octahedral pairs, centered around the center

Table 2. *Important bond distances* (Å) *and angles* (°)
for SmS$_6$ *octahedra in* BaSm$_2$S$_4$

Sm(1)S$_6$ octahedron

Sm(1)^e—S(1)^{b,f}	2.859 (3)	(2 ×)
Sm(1)^e—S(1)^g	2.802 (4)	
Sm(1)^e—S(2)^{b,f}	2.752 (3)	(2 ×)
Sm(1)^e—S(4)^e	2.813 (4)	
S(1)^{f,g}—Sm(1)—S(1)^{f,b}	86.35 (10)	(2 ×)
S(1)^f—Sm(1)—S(1)^b	92.2 (1)	
S(1)^{f,e}—Sm(1)—S(2)^{f,b}	85.36 (9)	(2 ×)
S(1)^g—Sm(1)—S(2)^{b,f}	91.15 (10)	(2 ×)
S(1)^{b,f}—Sm(1)—S(4)^e	91.01 (9)	(2 ×)
S(2)^f—Sm(1)—S(2)^b	97.0 (1)	
S(2)^{b,f}—Sm(1)—S(4)^e	91.38 (10)	(2 ×)
S(1)^{f,b}—Sm(1)—S(2)^{b,f}	176.62 (10)	(2 ×)
S(1)^g—Sm(1)—S(4)^e	176.2 (1)	

Sm(2)S$_6$ octahedron

Sm(2)^e—S(2)^h	2.803 (4)	
Sm(2)^e—S(3)^e	2.762 (4)	
Sm(2)^e—S(3)^{i,j}	2.812 (3)	(2 ×)
Sm(2)^e—S(4)^{a,k}	2.820 (3)	(2 ×)
S(2)^h—Sm(2)—S(3)^{i,j}	82.43 (9)	(2 ×)
S(2)^h—Sm(2)—S(4)^{a,k}	85.62 (10)	(2 ×)
S(3)^e—Sm(2)—S(3)^{i,j}	82.35 (9)	(2 ×)
S(3)^i—Sm(2)—S(3)^j	94.2 (1)	
S(3)^{i,j}—Sm(2)—S(4)^{k,a}	84.68 (9)	(2 ×)
S(3)^e—Sm(2)—S(4)^{a,k}	109.25 (9)	(2 ×)
S(4)^a—Sm(2)—S(4)^k	93.9 (1)	
S(2)^h—Sm(2)—S(3)^e	157.5 (1)	
S(3)^i—Sm(2)—S(4)^{a,k}	168.0 (1)	(2 ×)

Symmetry code: (*a*) to (*d*), see Fig. 1; (*e*) x, y, z; (*f*) $\frac{1}{2} - x, -y, \frac{1}{2} + z$; (*g*) $-\frac{1}{2} + x, \frac{1}{2} - y, \frac{3}{2} - z$; (*h*) $-\frac{1}{2} + x, \frac{1}{2} - y, \frac{1}{2} - z$; (*i*) $-x, -\frac{1}{2} + y, -z$; (*j*) $-x, \frac{1}{2} + y, 1 - z$; (*k*) $\frac{1}{2} - x, -y, -\frac{1}{2} + z$.

of the *ab* and *bc* planes (see below), share two other S atoms, 2 S(3). The two asymmetric SmS$_6$ pairs (double-octahedral units) further share S atoms S(2) and S(4) to extend the structure along the *ac* plane. The larger barium cation, Ba^{2+}, is accommodated between double-octahedral units. In Fig. 1, the barium coordination, eight, is outlined by dashed lines.

The polyhedral representation of the BaSm$_2$S$_4$ structure, projected onto the *ac* plane, is shown in Fig. 2. The double-octahedral units share edges of the SmS$_6$ octahedra. Each unit is joined by octahedral corners, S(2) and S(4) as mentioned above, to four other units. The double-octahedral units, adopted by two crystallographically independent Sm(1)S$_6$ and Sm(2)S$_6$ octahedral pairs, propagate along the *b* axis by sharing opposite edges of octahedra to form double-octahedral infinite chains. Each octahedron shares four edges with neighbouring SmS$_6$ octahedra. The Sm—S bond distances, as listed in Table 2, range from 2.75 to 2.86 Å, which is comparable with the sum, 2.80 Å, of Shannon crystal radii of six-coordinated Sm^{3+}, 1.098 Å, and S^{2-}, 1.70 Å (Shannon, 1976). Based upon the deviation of octahedral angles, it is noted that the Sm(2)S$_6$ octahedron is more distorted than Sm(1)S$_6$.

The above described eight-coordinated BaS$_8$ can be essentially viewed as a bicapped trigonal prism (b.t.p.), as shown in Fig. 3. The Ba atoms not only stabilize the three-dimensional framework but, moreover, complete the electrostatic neutrality for the coordinated S atoms. (Each S atom has five coordination with three Sm and two Ba atoms.) The two S atoms, 2 S(2), capping the square-planar faces of the t.p. adopt longer Ba—S distances, *e.g.*, 3.327 (4) and 3.425 (4) Å, which can be justified by the weak Ba—S(2) interaction, attributed to the nonstoi-
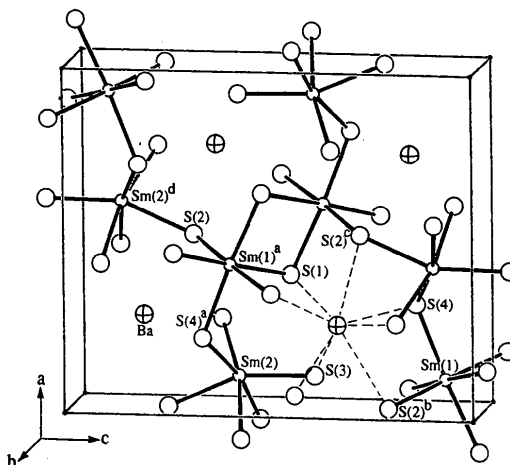

Fig. 1. An *ORTEP* (Johnson, 1976) drawing of the BaSm$_2$S$_4$ structure viewed approximately along the *b* axis. All the Sm atoms (small open circles) occur at $y = \frac{1}{4}$ and $\frac{3}{4}$. To complete the SmS$_6$ octahedral coordination, the S atoms (large open circles) are drawn at $\frac{1}{4}$ and $\pm \frac{1}{2}$ in y with respect to the Sm atoms. The four Ba atoms in the unit cell are shown as cross-hatched circles. Atoms are labeled according to the asymmetric unit reported in Table 1, with the extra symmetry codes: (*a*) $\frac{1}{2} - x, 1 - y, -\frac{1}{2} + z$; (*b*) $\frac{1}{2} - x, 1 - y, \frac{1}{2} + z$; (*c*) $1 - x, \frac{1}{2} + y, 1 - z$; (*d*) $\frac{1}{2} + x, \frac{1}{2} - y, \frac{1}{2} - z$.
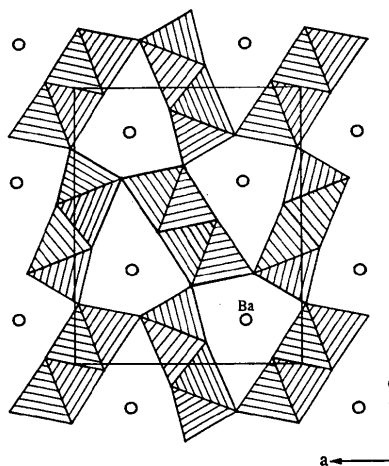

Fig. 2. A *STRUPLO* (Fischer, 1985) polyhedral representation of the BaSm$_2$S$_4$ structure projected along the *b* axis.
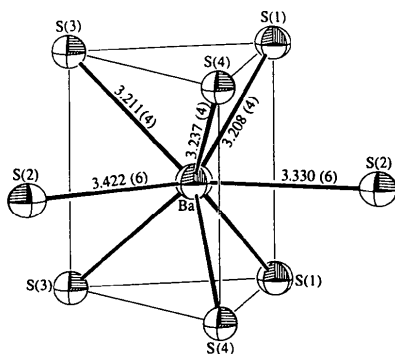
Fig. 3. An *ORTEP* drawing of the BaS_8 polyhedron shown in a bicapped trigonal prismatic configuration. The anisotropic atoms are presented at 90% probability. The Ba—S bond lengths are given in ångströms.

chiometry. Otherwise the t.p. Ba—S distances are in the range 3.21–3.24 Å, which is consistent with the crystal radii sum, 3.26 Å, of eight-coordinated Ba^{2+} (1.56 Å) and six-coordinated S^{2-} 1.70 Å, according to Shannon.

References

CARPENTER, J. D. & HWU, S.-J. (1991). *Chem. Mater.* Submitted.
CARPENTER, J. D. & HWU, S.-J. (1992). *J. Solid State Chem.* **97**, 332–339.
CROMER, D. T. & WABER, J. T. (1974). *International Tables for X-ray Crystallography*, Vol. IV, pp. 71, 148. Birmingham: Kynoch Press. (Present distributor Kluwer Academic Publishers, Dordrecht.)
DECKER, B. F. & KASPER, J. S. (1957). *Acta Cryst.* **10**, 332–337.
FISCHER, R. X. (1985). *J. Appl. Cryst.* **18**, 258–262.
JOHNSON, C. K. (1976). *ORTEP*II. Report ORNL-5138. Oak Ridge National Laboratory, Tennessee, USA.
MEISEL, K. (1939). *Z. Anorg. Allg. Chem.* **240**, 300–312.
PATRIE, M., GOLABI, S. M., FLAHAUT, J. & DOMANGE, L. (1964). *CR Acad. Sci. Paris*, **259**, 4039–4042.
Phase Diagrams for Ceramists (1969). Vol. II, edited by E. M. LEVIN, C. R. ROBBINS, & H. F. McMURDIE, Fig. 3053. The American Ceramic Society, Inc.
SHANNON, R. D. (1976). *Acta Cryst.* A**32**, 751–767.
TEXSAN (1989). *Single Crystal Structure Analysis Software*, version 5.0 Molecular Structure Corp., The Woodlands, TX, USA.
ZACHARIASEN, W. H. (1968). *Acta Cryst.* A**24**, 212–216.

Structure of the Fully Ferroelectric/Fully Ferroelastic Orthorhombic Room-Temperature Phase of Cobalt Bromine Boracite, $Co_3B_7O_{13}Br$ and Nickel Chlorine Boracite, $Ni_3B_7O_{13}Cl$

BY F. KUBEL, S. Y. MAO AND H. SCHMID

Département de Chimie Minérale, Analytique et Appliquée, Université de Genève, CH-1211 Genève 4, Switzerland

Abstract. The X-ray crystal structures of optically controlled single-domain crystals of fully ferroelectric/fully ferroelastic cobalt bromine boracite, $Co_3B_7O_{13}Br$ (Co–Br) at 298 K [$M_r = 540.38$, orthorhombic, $Pca2_1$, $a = 8.5614$ (2), $b = 8.5657$ (2), $c = 12.1196$ (3) Å, $V = 888.78$ (4) Å^3, $Z = 4$, $D_x = 4.04$ Mg m^{-3}, λ(Mo $K\alpha$) = 0.7107 Å, $\mu = 10.61$ mm^{-1}, $F(000) = 1020$, $R = 7.0$, $wR = 5.4\%$, 2824 reflections] and of nickel chlorine boracite, $Ni_3B_7O_{13}Cl$ (Ni–Cl) at 298 K [$M_r = 495.25$, orthorhombic, $Pca2_1$, $a = 8.5105$ (4), $b = 8.4984$ (4), $c = 12.0324$ (5) Å, $V = 870.25$ (7) Å^3, $Z = 4$, $D_x = 3.78$ Mg m^{-3}, λ(Mo $K\alpha$) = 0.7107 Å, $\mu = 6.8$ mm^{-1}, $F(000) = 960$, $R = 3.5$, $wR = 3.1\%$, 2082 reflections] are reported. The metal surroundings of Co–Br and Ni–Cl were analyzed in detail and show two metal sites (Co2, Co3; Ni2, Ni3) with chemically similar environments and one metal site (Co1; Ni1) with a different environment. Six B atoms have a tetrahedral or slightly distorted tetrahedral coordination, whereas one B atom (B4) has triangular surroundings in both compounds.

Introduction. Cobalt bromine boracite and nickel chlorine boracite undergo respective improper phase transitions at 466 and 608 K from a cubic